RSC Advances

ROYAL SOCIETY OF CHEMISTRY

www.rsc.org/advances

Co-delivery of siRNA and paclitaxel into cancer cells by hyaluronic acid modified redox-sensitive disulfide-crosslinked PLGA-PEI nanoparticles†

Yan Shen[a#], Jue Wang[b#], Yanan Li[a], Yu Tian[a], Huimin Sun[b], Ouahab Ammar[d], Jiasheng Tu[a], Wang Buhai[c*],Chunmeng Sun[a*]

[a]State Key Laboratory of Natural Medicines, Department of Pharmaceutics, School of Pharmacy, China Pharmaceutical University, 24 Tong Jia Xiang, Nanjing, China

[b] National Institute for Food and Drug Control, Beijing, People's Republic of China

[c]Department of Oncology, Subei People's Hospital, Yangzhou, China

[d]Department of Pharmacy, Institute of Medical Sciences. Batna Elhadj Lakhdar University

[*]Corresponding author. Tel: +86-025-83271305. Suncm_cpu@hotmail.com (C. Sun) and wbhself@sina.com (B. Wang).

† Electronic Supplementary Information (ESI) available: Characterization of DTX / siRNA /HPP and DTX/siRNA /HRPSP nanoparticles , Cellular uptake studies ,Tumor-targeting properties of complexes observed by in vivo imaging .

Abstracts：

The main objective of our research was established in order to put forward a targeted anticancer co-delivery system for both micro-molecularchemotherapeutic drugs and small interfering RNA (siRNA). The drug delivery system can efficiently combine the advantages of the two therapeutic strategies with different mechanisms via their synergetic effects for cancer therapy. In this study, A cooperative nano-platform of docetaxel (DTX) and specific silencer select siRNA was developed; suppressing the cyclooxygenase-2(COX-2) gene expression within one single nano-particle (NP) composed of poly(D,L-lactide-co-glycolide) (PLGA) bearing disulfide-linkaged reducible polyethyleneimine (PEIss) covered by hyaluronic acid (HA). PEIss was successfully synthesized by Michael addition of low molecular weight PEI (Mw=1800Da) with cystaminebisacrylamide (CBA). Docetaxel (DTX) was entrapped into the hydrophobic PLGA core, while negatively charged siRNA was adsorbed on the cationic shell of PEIss by electrostatic attraction. The redundant positive charge of PEIss allowed the introduction of HA onto the nanoparticles as active targeting groups. The whole complex was then delivered to both sensitive and resistant SGC-7901 gastric cancer cells that over-express CD_{44} receptors. This novel system was designatedas HRPSP NPs(HA-PEIss-PLGA nanoparticles). HA-PEI-PLGA nanoparticles (HPP NPs) were also prepared to make a comparison. The electrophoresis confirmed the good stability of siRNA/HRPSPcomplex in the presence of PBS(pH7.4), competitive heparin and RNase and remarkable sensitivity and reducibility to GSH. In in-vitro cell transfection, siRNA/HRPSP complexes performed higher transfection efficiency than siRNA/HPP and siRNA/RPSP and siRNA/PP complexes preferentially through caveolae-mediated endocytosis, which might be a desirable pathway to avoid the lysosomal

degradation of delivered genes. Q-PCR and Western Blot experiments proved that COX-2 mRNA and COX-2 protein expressions were reduced to a statistically significant level in comparison with the control and the scrambled HRPSP/siRNAcomplex after treatment with NPs/siRNA complex. In vivo , Dir/HRPSP/ siRNA NPs complexes exhibited higher intensity at the tumor tissue compared to the non HA modified complexes. The biodistribution results demonstrated that DTX/HRPSP NPs could reduce DTX uptake by particularly the liver and lungs to limit the side effects while significantly increasing DTX accumulation in the tumors. Above these, HRPSP NPs were highly promising nano-carriers for the combinatorial delivery of siRNA and lipophilic anti-cancer drugs.

Keywords:targeted delivery; redox-sensitive; siRNA; hyaluronic acid; co-delivery; DTX; COX-2

1. Introduction

Nowadays, cancer treatments face many challenges as a consequence of high systemic toxicity caused by high dose administration and multidrug resistance following regular chemotherapy or coordinated treatment of several drugs administered by different routes[123]. The progression of cancer involves complex dynamic changes in the genome and a complicated network of interactions in cancer cells with multiple distinct cell types that form tumors[4]. As a result, novel drug delivery strategies using combination therapy of two or more agents in one single carrier based on nano-sized drug delivery systems (DDS) including cationic polymeric micelles, nanoparticles and liposomes[5,6,7]. which have been prosperously developed in the treatment of many types of cancer. DDS for co-delivery of several agents possessing targeting moiety increases their selective accumulation at the tumor site and enhances their activity allowing administration of lower doses of each agent, thus reducing their side effects. The combinational therapies may cover small molecules, proteins, small interfering RNA (siRNA) or microRNA(miR). Recent research proved that the combination treatments with chemotherapeutics have high efficiency due to their ability to affect multiple disease pathways and distinct mechanisms[8].

Small interfering ribonucleic acid (siRNA) technology provides new types of drugs that are easily designed and have high target selectivity to inhibit specific gene expression in the cytoplasm[9]. So far, the potential of siRNA-based therapeutic strategies for cancer has been demonstrated in breast cancer, prostate cancer, cervical cancer, nasopharyngeal carcinoma, leukemia, and ovarian cancer, as well as viral infections[10]. COX-2 protein is overexpressed in above cancer cells , induce angiogenesis , inhibit apoptosis and play a important role in the growth of tumor[11,12,13,14,15] , which is a target in tumor therapy. However, the major limitations of their inherent rapid degradation, poor cellular uptake and poor tissue specificity in the delivery of siRNA are still barriers demanding prompt solution[16]. Nanocarriers are usually favorable in siRNA delivery because they can stably encapsulate, complex, protect and selectively deliver siRNAs to target tumor tissues and cells[17,18]. At the same time, engineered nanocarriers can combine traditional small chemical drugs with siRNA into one module so that they would produce faster anticancer effect during their intracellular uptake; or overcome multidrug resistance (MDR) with targeting abilities and minimized side-effects. Complexed with anti-COX2 siRNA by NPs could induce apoptosis of the tumor cells by enhanced EPR effect[19]. Dawen Dong found that combining gene therapy with chemotherapeutics is more effective than treatment of cancer with individual delivery systems carrying either gene or drug by a a multifunctional folate-decorated and pH-responsive nanocomplex[20]. Furthermore, synergistic combinations of several types of therapeutic approaches with distinct mechanisms can overcome the toxicity and other side effects associated with high doses of single drugs and have more to be researched[21,22].

We constructed a co-delivery nano system based on PLGA-PEIss nanoparticles covered by hyaluronic acid (HA) to combine siRNA

suppressing COX-2 (siCOX-2) gene expression and docetaxel (DTX) in order to target SGC-7901 cells. PLGA is used as the hydrophobic core of the nanoparticle which is considered as a cargo of DTX, PEIss as the cationic shell and HA as the active targeting group (Fig.1). HA is biodegradable, non-toxic, nonimmunogenic and non-inflammatory, which makes this polymer an ideal carrier for systemic drug delivery applications. What is more important is that lots of research have proven that HA backbone in itself possesses tumor targeting moieties that specifically recognize CD_{44} receptors over-expressed on certain surfaces of tumor cells [23,24]. PEIss is a reconstructed cationic polymer from commercial branched polyethyleneimine (Mw 1.8kDa), cross-linked by disulfide which is sensitive to high concentration of glutathione (GSH) in tumor cells which consequently facilitates and controls the release of siRNA. Based on the above properties of the materials, the co-delivery of gene and drug by HA-PEIss -PLGA NPs which is sensitive to the microenvironment of tumor have not been investigated by other groups. In our studys, a cooperative nano-platform of docetaxel (DTX) and specific silencer select siRNA was developed; suppressing the cyclooxygenase-2 (COX-2) gene expression. The properties of the nanoparticles were characterized, and the ability of the nanocomplex to simultaneously deliver siRNA and DTX into the same tumor cells was examined, and the targeting effect in vivo was investigated for further reduction and induce apoptosis of cancer cells.This study demonstrated that HRPSP NPs were highly promising nano-carriers for the combinatorial delivery of siRNA and lipophilic anti-cancer drugs.

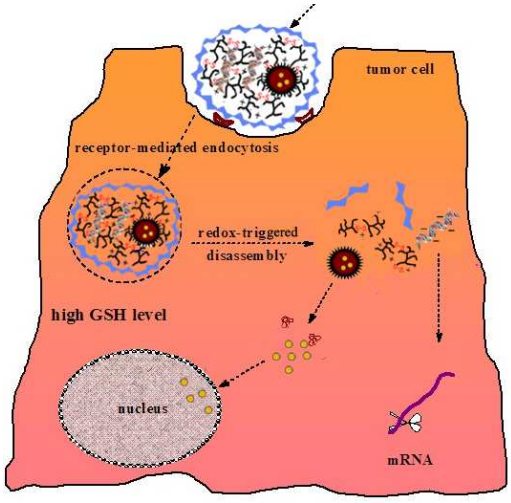

Fig.1. Schematic diagram showing the structure of the co-delivery nano-complex and the process of entering tumor cells.

Experimental section

Materials

Poly(D,L-lactide-co-glycolide) (PLGA, lactide:glycolide ratio 50:50； Mw,10kDa) was purchased from Shandong Daigang Chemical Reagent Co.,Ltd. (Jinan, Shandong, China). Branched Polyethyleneimine (PEI, Mw1.8kDa and 25kDa) was from Alfa Aesar, A Johnson Matthey Company. N,N'-cystaminebisacrylamide (CBA) was obtained from Sigma-Aldrich Corporation (St. Louis, MO). Human siRNA targeting COX-2 massager RNA labled with carboxyfluorescein (FAM) (sense: 5'-AAGTGCGATTGTACCCGGACA-3';) and control siRNA

(non-silencing) (sense: 5'-GACTTCATAAGGCGCATGC-3';) were synthesized by GenePharma Co., Ltd. (Shanghai, China). siRNA labeled with Alexa488 (λ_{ex}= 495 nm,λ_{em}= 519 nm) at the 5 ′end of the sense strand were also purchased from GenePharma Co., Ltd. (Shanghai, China), Pluronic F68 was kindly provided from BASF Corporation (Mount Olive,NJ,USA), Poly(vinyl alcohol)(PVA) was purchased from Wanqing Co., Ltd. (Nanjing, China). Sodium hyaluronate (Mw 11 kDa) was purchased from Freda Biochem Co., Ltd. (Shandong, China).

MTT ((3-(4,5-dimethyl-thiazol-2-yl)-2,5-diphenyl-tetrazolium bromide), HME mesangial cell lines and Human gastric adenocarcinoma cell lines SGC 7901 were obtained from Shanghai Institute of Cell Research (Shanghai, China). Fetal bovine serum (FBS), Dulbecco's modified Eagle's medium (DMEM) and RPMI 1640 medium were purchased from Gibco BRL (Grand Island,NY). RNase-free distilled water, DAPI, Lipofectamine, LysoTraker Red® and SYBR®gold (nucleic acid gel stain) were purchased from Invitrogen (Carls-bad, CA). Phenylarsine oxide (phAsO), amiloride, filipin III from Streptomyces filipinensis , DiR(1,1'-dioctadecyl-3,3,3',3'-tetramethyl indotricarbocyanine Iodide) were from Sigma Chemical Co., Ltd. (Saint Louis, MO). All other chemicals and reagents were of analytical grade.

Animal use

All animal were purchased from qinglongshan farms (Nanjing, China). All animal experiments were conducted in full compliance with the National Institute of Health Guide for the Care and Use of Laboratory Animals and approved by the Animal Ethics Committee of China Pharmaceutical University.

Cell culture and cell lines

The SGC-7901 gastric cancer cells and HME mesangial cells were used. HME mesangial cells and SGC-7901 cells were cultured in RPMI1640 medium with 10% fetal bovine serum (FBS) at 37 °C in5% CO_2 atmosphere. All culture media were replaced every two days.

Synthesis of disulfide-containing polyethyleneimine with cystaminebisacrylamide(CBA)

Reducible polyethyleneimine containing disulfide bond (PEIss) was synthesized by Michael addition where N,N'-cystaminebisacrylamide (CBA) was used as disulfide provider. PEI (2g) and CBA (0.15g,0.18g, 0.24g,0.3g) were separately dissolved in 12ml and 8ml of methanol (80%), and then CBA was added into the PEI at 1ml/30min in a three-necked flask equipped with a condenser. N_2 was allowed into the flask to thoroughly replace the air. The reaction was initiated at 55°C in the dark with successive stirring for three days. Subsequently, the organic solvent was evaporated by a rotary evaporator. Ultrafiltration with a molecular weight cut-off of 3500Da was used to get rid of low molecular weight PEI, then the solution was lyophilized for dehydration. The confirmation of disulfide linkage was determined by ^{1}H-NMR and the molecular weight was measured by gel exclusion chromatography (GPC).

Preparation of DTX-loaded siRNA/HPP and siRNA/HRPSP nanoparticles

HA-PEI-PLGA nanoparticles (HPP NPs) and HA-PEIss-PLGA nanoparticles (HRPSP NPs) embedding DTX were first prepared by emulsion-diffusion-evaporation method. Briefly, 9 ml of an organic phase containing 0.2g of PLGA, 2mg of DTX in 6.5ml of acetone and 2.5ml of dichloromethane were mixed with 1ml solution (20mg/ml) of PEI (or PEIss) in acetone (or distilled water). The mixture was then slowly poured onto 10 ml of PVA aqueous solution (3%,w/v) or 10ml of polyxamer188 aqueous solution (5%,w/v) and then sonicated for

20min (195 W) in an ice bath using an ultrasound probe. The dichloromethane and acetone were then evaporated under vacuum using a rotary evaporator at 37 °C for 10 min. The obtained micellar PEI-PLGA nanoparticles (PP NPs) or PEIss-PLGA nanoparticles (RPSP NPs) were stored at 4 °C. DTX/siRNA /HPP and DTX/siRNA /HRPSP complexes were prepared according to various nitrogen/phosphorous (N/P) ratios. N/P ratios were calculated assuming that 43g/mol corresponds to each repeating unit of nitrogen atom (N) in PEI (or PEIss) polymer, while 330g/mol corresponds to each repeating unit of phosphorous atom (P) in siRNA. The resulting proportions of PEI and siRNA in the coexisting complex are expressed as N/P ratios. Hyaluronic acid (HA) was adsorbed onto the complexes just by simple mixing along with vortex, then incubating them at room temperature for 15min. Various amounts of HA were used to form nanoparticles with different surface charges.

Characterization of DTX / siRNA /HPP and DTX/siRNA /HRPSP nanoparticles

The particle size, size distribution and zeta potential of DTX/siRNA /HPP and DTX/siRNA /HRPSP NPs in HEPES buffer solution with various N/P /COOH ratios or N/P ratios were measured using a Malvern Zetasizer Nano-ZS90 (Malvern instruments, UK). All of the dynamic light scattering (DLS) measurements were performed at 25°C and at a scattering angle of 90° detection angle. The morphology and size distribution were observed by transmission electron microscopy (TEM, H-600, Hitachi, Japan).

Buffering capacity

Buffering capacity was determined by acid–base titration as described with some modifications [25]. Briefly, 0.02 mg/ml of each sample solution (PEI_{1800}, PEI_{25K}, PEIss (m_{CBA}:$m_{PEI1800}$=0.09, 0.15) was prepared by dissolving the polymer in 5ml of 150mM NaCl solution, and then the pH was set to12.0 using 1N NaOH. The pH change was recorded with the increasing volume of HCl titrant (0.01N). The consumed volume of HCl in the pH interval from 7.4 (extracellular environment) to 5.1 (the late endosomal environment) can be used to evaluate protonated capacity of protonable nitrogen in the polymer. For comparison, PEI 25K and PEI 1.8K were also titrated using the same method. The buffer capacity was calculated referring to the formula[26] as follows:

$$\text{Buffer Capacity (\%)} = \frac{\left(\Delta V_{\text{sample}} - \Delta \text{NaCl}\right) \times 0.01M}{\text{mol } N} \times 100\%$$

ΔV_{sample}, Δ_{NaCl} : the volumes of HCl titrant (0.01N) added to change the pH from 7.4 to 5.1 in the polymer solution and pure150mM NaCl solution. Mol N: the total amount of protanable nitrogen atoms in the polymer.

Stability of siRNA /PP , siRNA /HPP , siRNA /RPSP and siRNA /HRPSP nanoparticles

The binding ability of siRNA adsorbed onto the four types of nanoparticles was determined by the electric mobility of siRNA into a 2% agarose gel. A series of different N/P ratios and N/P/COOH ratios of NPs (10μl of the sample containing 0.4μg of siRNA) were prepared and then added to each well. The electrophoresis was carried out at a constant voltage of 85 V for 30min in TBE buffer (4.45mMTris-base, 1mM sodium EDTA, 4.45mM boric acid, pH8.3) containing 5μl SYBR®gold. The siRNA bands were then visualized under a UV trans-illuminator at a wavelength of 254 nm (Bio-Rad®, Marnes-lacoquette, France). For complex anti-anion stability study, PP/siRNA NPs, RPSP/siRNA NPs with N/P=10/1, HPP/siRNA NPs and HRPSP/siRNA NPs with N/P/COOH=10/1/24 (10μl of the sample containing 0.4μg of siRNA) were prepared and then incubated at room temperature for 20min. different amounts of heparin ($m_{heparin}$:m_{siRNA}, μg /μg =0.1,0.2,0.3, 0.4,0.5, 1,2)

were added into the complexes and then incubated for another 20min at room temperature. For complex anti-enzymes stability study, 40μg/ml of RNase was added into the complexes and then incubated at 37 °C for different time intervals (0, 5min, 15min,, 30min, 60min, 120min and 240 min). At the end of the predetermined time, 1μl of heparin (10%) was added to the complexes to set the undamaged siRNA free. Naked siRNA was used as the negative control. The next procedure was conducted as earlier. The intact siRNA percentage was calculated based on the relative intensity of free siRNA band in each well with respect to wells with free siRNA (i.e., in the absence of any conjugate). The binding for each conjugate was tested at least in 3 independent experiments.

Redox sensitive release of siRNA /PP, siRNA /HPP , siRNA /RPSP and siRNA /HRPSP nanoparticles

Disulfide bond can be deoxidized by high concentration of glutathione in tumor cells, the absorbed siRNA is released into the cytoplasm. To testify the reductable sensitivity of PEIss and the property to control the release behavior in tumor cells; RPSP/siRNA complex with N/P=10/1 and HRPSP/siRNA complex with N/P/COOH=10/1/24 were freshly prepared, and then added with GSH (60μg/μl) 1μl, incubated at 37 °C for 24h. Before electrophoresis different concentrations of heparin were added into 1μl of mixture to obtain 10μl of total volum. At the same time, PP/siRNA complex and RPSP/siRNA complex were measured for comparison. The next procedure was performed as described in section 2.6.

MTT assay

The cytotoxicity of PP, HPP, RPSP and HRPSP NPs was evaluated using the MTT (3-(4,5-dimethylthiazol- 2-yl)-2,5 -diphenyltetrazolium bromide) colorimetric test by calculating the cell viability percentage. SGC-7901 cells and HME mesangial cells were seeded in a 96-well plate at a density of 5000 cells per well in RPMI1640 medium containing 5% FBS and grown overnight respectively. After 24h incubation of serial concentrations of the four types of NPs in each well at 37 °C for 24h, 20μl of MTT (5mg/ml) was added to each well and then incubated for 4h at 37 °C to form formazan crystals. The medium was removed before 150ul of dimethyl sulfoxide (DMSO) was added to each well. The plate was shaken slowly for 10min to dissolve the formazan dye completely. Comparison was performed under the same condition. The absorbance of dissolved formazan was measured at 570nm using Microplate Reader. Cell inhibition percent was calculated as the following formular:

$$\text{Cell inhibition (\%)} = \left(1 - \frac{OD_{\text{sample}} - OD_{\text{blank}}}{OD_{\text{sample}}}\right) \times 100\%$$

OD_{sample}: the absorbance of formazan in live cells incubated with nanoparticles; OD_{blank}: the absorbance of the blank sample.

The toxicity of the four types of nanoparticles was expressed as the inhibitory concentration at which 50% of cell growth inhibition was obtained (IC_{50}).

Cellular uptake studies

Intracellular delivery of siRNA /PP, siRNA /RPSP, siRNA/ HPP and siRNA /HRPSP NPs

4×10^4 or 5×10^4 SGC7901 cells were seeded in 24-well plates 20h in advance before adding different N/P ratios or N/P/COOH ratios of complexes with Cy3 or FAM labeled siRNA into the wells. The siRNA concentration was constant at 100nM per well. After incubation at

37 °C for 16h, PBS (pH7.4) was used to wash the cells three times. 4% paraformaldehyde was added to fix the cells at room temperature for 20min, and then the cells were treated by 1μg/ml diamidino-phenyl-indole (DAPI) for 10min to locate the cell nucleus. Lipofectamine® was used as positive control. Finally, all the cell samples were washed with PBS for three times and observed under the Fluorescence Inversion microscope for similar confluency and morphology (Nikon TE2000, JP) at an excitation wavelength of 488nm. To determine the transfection efficiency, the cells were washed twice and lysed with Trypsin–EDTA solution and analyzed by FACS Calibur flow cytometer (BD, Biosciences, USA).

To investigate whether HPP and HRPSP/siRNA complexes were specifically taken up by SGC 7901 cells through HA receptor (CD_{44}) mediated endocytosis, an excess amount (10 mg/ml) of HA (10K) was added to the transfection medium to block the interaction between HPP or HRPSP/siRNA complexes and HA receptor on the cell surface. 1 mg of HPP and HRPSP/siRNA complexes were post-transfected in the presence of 10 mg of HA. After 12 h, transfected cells were trypsinized and washed three times with PBS and fixed with 1% paraformaldehyde solution. The transfection efficiency of HPP or HRPSP/siRNA complexes in the presence of free HA was monitored by flow cytometry as described above. Fluorescent signals were measured on a Mithras LB 940, corrected for background signals and expressed as relative to the signal of free siRNA. Generally, a minimum of 2×10^4 cells was analyzed in each measurement. All experiments were performed in triplicates.

Mechanism of cellular uptake studies

To investigate whether the intracellular uptake was energy dependent and in which way the RPSP/siRNA and HRPSP/siRNA NPs entered SGC-7901 cells, the cells were pretreated in the presence of such different uptake inhibitors as NaN_3/2-DG(energy-dependence inhibitor), filipin (1mg/ml, inhibitor of caveolae-mediated endocytosis), aminorin（5mM,1.33mg/ml, inhibitor of macropinocytosis), and PhAsO (inhibitor of clathrin-mediated endocytosis) in serum-free media for 30 min at 37°C. After washing with PBS three times, either the FAM-siRNA/RPSP NPs (N/P=40) or the FAM-siRNA/HRPSP NPs (N/P/COOH=40/1/2) were added in the culture medium and incubated for 24h at 37°C before cells were treated for the measurement by FACS Calibur flow cytometer (BD, Biosciences, USA). Cells with no any pretreatment were taken as a control. The cells then were trypsinized and collected into an Eppendorf tube. The cells then were washed twice after pelleting by centrifugation (1500 rpm, 4°C, 5 min) and were suspended in 1 mL of heparin–PBS. Finally, cells were suspended in 0.5 mL of PBS and filtered through a nylon mesh. The cells then were analyzed by FACS Calibur flow cytometer (BD, Biosciences, USA) above. All experiments were performed in triplicates.

Gene silencing study

TaqMan real-time reverse-transcription and quantitative PCR (RT-qPCR)

Total RNA was isolated from monolayer culture of SGC-7901 pre-transfected with either 50 nM of siCOX-2 only (negative control), scrambled siRNA only, scrambled siRNA /Lipofectamine®, siCOX-2/Lipofectamine®, siCOX-2/PP, siCOX-2/HPP, siCOX-2/PRSP, and siCOX-2/HPRSP NPs for 24h using a Trizol solution. Briefly, 1ml of Trizol solution was added to the constructs and homogenized thoroughly. 200 μl of chloroform was added to the homogenate with vortexing and then incubated at room temperature for 5 min. The homogenate was centrifuged at 4 °C for 15 min at 15000 ×g. An aqueous phase was separated with the addition of 500 μl of cold isopropanol and incubated for 10 min at room temperature. Samples were centrifuged at 4 °C for 10 min at 15000 ×g and the RNA pellet was obtained. The RNA pellet was

diluted with DEPC water to adjust the RNA concentration. The transcription was completed with EzOmics^{TM} One-Step qPCR Kit (Baiao Co. Lid,China). SYBR Green I was used to finish the qPCR analysis targeting COX-2 and β-actin. Analysis was performed using the Applied Biosystems Step One Real-Time PCR Systems. Relative gene expression values were determined by the DDCT method using Step One Software v 2.1 (Applied Biosystems). Data are presented as the fold difference in COX-2 expression normalized to the house keeping gene β-actin as the endogenous reference, and relative to the untreated control cells. Primers used in qPCR for COX-2 and β-actin are:

COX-2 forward：5'-GAAGGTGAAGGTCGGAGTC-3'

COX-2 reverse：5'-GAAGATGGTGATGGGATTTC-3' and

β-actin-forward： 5'-GAAGGTGAAGGTCGGAGTC-3'

β-actin-reverse：5'-GAAGATGGTGATGGGATTTC-3'

PCR parameters are as follows: Taq activation at 95°C，followed by 35 cycles of PCR at 95°C，15s，60°C，1min and 1 cycle of 95°C, 15s, 60°C, 1min, 95°C, 15s and 60°C,15s. Standard curves were generated and the relative amount of COX-2 mRNA was normalized to β-actin mRNA. Specificity was verified by melt curve analysis.

Western blot analysis of COX-2 protein

SGC-7901 cells were incubated in NP-40 lysis buffer containing 50 mM Tris (pH 7.4), 150 mM NaCl, 1 mM EGTA, 1% NP-40, 0.25% SDS, 1 mM sodium vanadate, 1 mg/ml protease inhibitors, 200 μg/ml chymostatin and 1 mM PMSF for 30 min at 4 °C. Cell lysates were then centrifuged at 14,000 rpm for 10 min and supernatants were harvested. An aliquot of 10 mg of lysates was boiled and electrophoresed in 7.5% SDS-polyacrylamide gels under reducing conditions. The separated proteins were then electrophoretically transferred to a PVDF membrane (Immoblin-P, Millipore, Bedford, MA, USA). Following the reaction with a blocking solution of 10% non-fat dried milk for 1 h at room temperature, the membrane was probed with an anti-COX-2- specific antibody (Santa Cruz Biotech, Santa Cruz, CA, USA) or anti-β-actin antibody (Santa Cruz Biotech, Santa Cruz, CA, USA) at room temperature for 1 h. After washing with Tris-buffered saline containing 0.05% Tween-20 and incubation with horseradish peroxidase-conjugated secondary antibodies, protein bands were detected by the enhanced chemiluminescence method (Amersham Life Science, Piscataway, NJ, USA). The gene silencing efficiency (%) was calculated based on the relative intensity of protein band of control group in each well with respect to wells with protein band of transfection groups. The COX-2 expression was normalized with β-actin gene expression. The gene silencing efficiency (%) for each transfection group was tested at least in 3 independent experiments.

Tumor-targeting properties of complexes observed by in vivo imaging

To evaluate the tissue distribution and targeting ability of siRNA/HRPSP NPs, 1,1'-dioctadecyl-3,3,3',3'-tetramethyl indotricarbocyanineiodide(Dir), a near infrared (NIR) fluorescent dye was encapsulated instead of DTX into PP, HPP, RPSP and HRPSP NPs with 0.2mg/ml of the final concentration. A certain amount of the Dir-loaded NPs was swirled with siRNA and added slowly dropwise. After incubation at room temperature for 10min, HA (10mg/ml) was also added slowly into the complex in the same way. Finally, a complex (N/P/COOH ratios =40/1/2) was prepared and kept at 4°C until use.

Approximately 1×10^6 SGC 7901 cells were inoculated subcutaneously in the armpit region of BALB/c nude mice (seven weeks old, 20-25 g). Tumors were allowed to grow to 1-2cm^3 in diameter for 2-3 weeks. Dir-loaded NPs were injected into the tail vein of tumor-bearing

mice at a dose of 1.25mg Dir/kg to investigate their tissue distribution and tumor-targeting efficacy in live mice. NIRF imaging experiments were performed at 2h, 4h, 6h and 8h post-injection. After the mice were sacrificed, their main organs including heart, liver, spleen, lung, kidney and the tumor were harvested . The in-vivo and in-vitro fluorescence intensity was determined by a Kodakin in vivo imaging system FX PRO (Kodak, USA) equipped with an excitation band pass filter at 720 nm and an emission at 790 nm. Images were analyzed using the Kodak Molecular Imaging Software 5.X. All experiments were conducted in strict accordance with the National Institute of Health Guide for the Care and Use of Laboratory Animals.

In vivo Biodistribution study

The biodistribution studies were performed on nude mice bearing SGC7901 tumors: SGC7901 cells (2×10^5 cells/50 ml media) were subcutaneously inoculated into the shaved right lateral flank of nude mice, and the study was initiated when the tumors reached 300-500mm^3 volume. All animals were fasted overnight before the experiment but allowed free access to water. Animals were randomly divided into four groups containing six animals per group. Mice were injected via the tail vein with DTX/PP, DTX/HPP,DTX/RPSP or DTX/HRPSP NPsat at an effective DTX dose of 40 mg/kg and at predetermined time points (10min,1h , and 12 h) blood was collected from the terminal cardiac puncture with heparinized tubes and plasma was separated by centrifugation (1500 ×g for 5 min). Then the mice were euthanized by cervical dislocation, and the tumor, heart, liver, spleen, lung, and kidney were harvested and rinsed with buffer and stored at -80°C until analysis. The mentioned organs were weighed after washing with NaCl 0.9%. The sectioned tissues and tumors were then homogenized (Ultra-Turrax, IKA T-18, Germany) and centrifuged for 10 min while methanol (1:1) was added for protein precipitation. The DTX amount in the supernatants was analyzed by HPLC as described above. Drug concentration values are described as ng DTX/mL plasma or ng DTX/g tissue. All data expressed as mean standard deviation (SD) represent of at least three or six different experiments. The difference between two groups was evaluated using Student t-test. A P value less than 0.05 was considered statistically significantly different.

Statistical analysis

Statistical analysis was performed using a standard Student's t-test (comparing only two individual groups) with a minimum confidence level of 0.05 for significant statistical difference. All values are reported in term of mean and standard deviation.

Results and Discussion

Synthesis of disulfide-containing polyethyleneimine (PEIss) with N,N'-cystaminebisacrylamide (CBA)

Reducible PEIss (RPS) composed of branched polyethyleneimine (PEI, 1.8kDa) and N,N'-cystaminebisacrylamide (CBA) was successfully synthesized by Michael addition reaction in four weight ratios: 0.075:1(R1), 0.09:1(R2), 0.12: 1(R3), 0.15: 1(R4). After purification the yield was more than 60%. The final product was viscous and soluble in water. 1H-NMR spectroscopy confirmed the structure of RPS as shown in Fig.2. The peaks for methyl protons, δ=3.07ppm [–S-CH2–](a), δ=3.47 ppm [–CO-NH–CH2–](b) and the peaks for ethyl protons, δ=2.39ppm

[-CH2-CH2-](c) of CBA clearly appeared in the spectrum. The molecular weight of synthesized RPS was determined by Gel Permeation Chromatography (GPC) as showed in Tab.2.

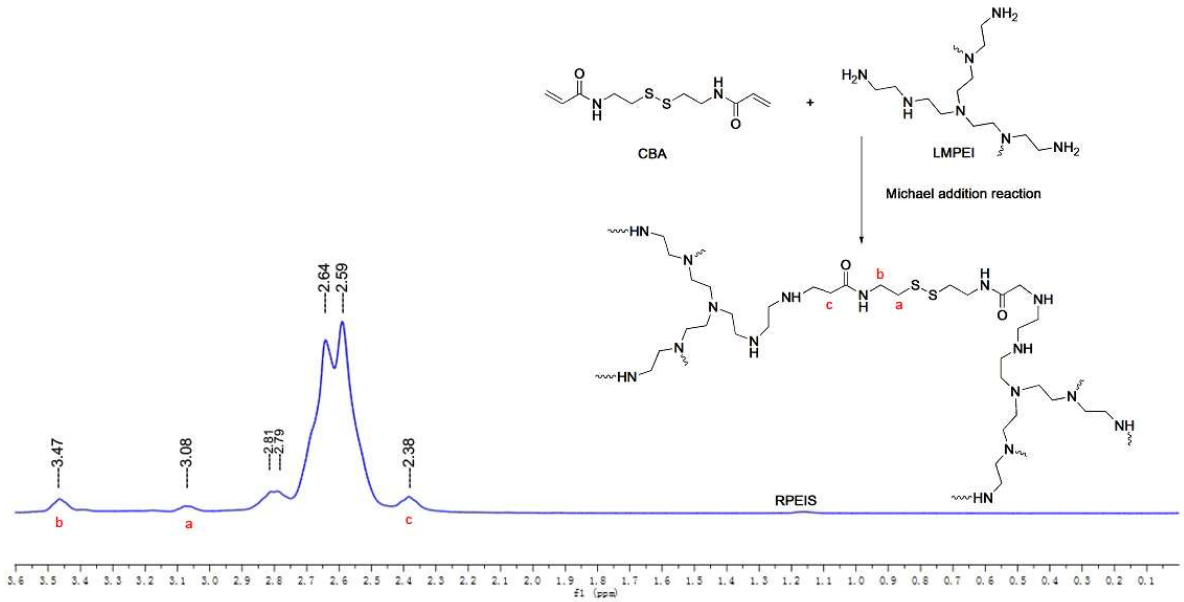

Fig.2 1H-NMR spectrum(300MHz) of RPS in D2O: The peaks for methyl protons, δ=3.07ppm [–S-CH2–] (a),δ=3.47 ppm [–CO-NH–CH2–](b), and the peaks for ethyl protons, δ=2.39ppm [-CH2-CH2-] (c).

Tab.1 Integral value to 1H NMR for figure 2

	Integrals	
Range	Normalized	Absolute
3.99-1.2.2	34.76	173790.46
3.55-3.41	1.00	4999.23

Buffer capability

Generally, the effects of the highly positively charged NPs on endolysosomal escape are mainly defined as the proton sponge effect, by determining the buffering capacity. PEIss 0.15:1 (mCBA: mPEI) showed a remarkable pH-buffering effect (proton sponge effect) for neutral to acidic conditions (Fig. 3). In other words, RPS (R4, 50kDa) are able to absorb protons at endolysosomal pH as the second-stage pH response, leading to an increase in osmotic pressure inside the endolysosomes, followed by membrane disruption and R4 release into the cytoplasm. Table 3 shows synthetic RPS with different ratios of CBA and PEI, has different buffer capability with PEI (~25kDa) and it seems that molecular weight is the main factor that influences the buffer capability of PEI or RPS. Since R4 showed a remarkable pH-buffering effect ($P<0.01$), this polymer would be used in the following experiments as PEIss.

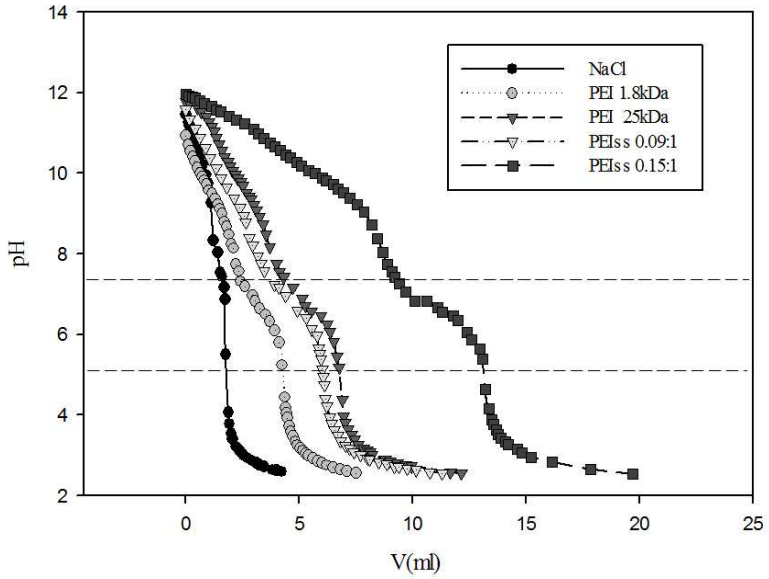

Fig.3 Acid-base titration profile of commercial PEI (1.8kDa, 25kDa) and RPS (R_2, R_4) . X-axis: the volume of HCl .

Tab2. Acid-base titration results of reference PEI and synthetic RPS.

	PEI(1.8kDa)	PEI(25kDa)	RPS(R_2, 23kDa)	RPS(R_4, 50kDa)
Buffer Capability (%)	10.55	13.76	13.47	22.07**

Note: P<0.01, vs PEI (1.8kDa)

Tab.3 Molecular weight of RPS calculated from GPC

Number	Weight ratios (CBA:PEI, w/w)	M_w(Da)	Mw/Mn
R_1	0.075:1	20498	1.57
R_2	0.09:1	22546	1.72
R_3	0.12:1	27634	1.90
R_4	0.15:1	50657	1.70
P_5	PEI	24799	2.89

P5:commercial PEI (Mw~25kDa)

Characterization of DTX / siRNA /HPP and DTX/siRNA /HRPSP nanoparticles

The surface properties of siRNA/NPs were investigated for morphology, particle size and zeta potential. S1 showed the representative morphology of DTX/siRNA/PRPS NPs and DTX/siRNA/HPRPS NPs through TEM. These NPs had a spherical shape and exhibited a core–shell structure with a uniform size of 50~100nm and 100~150nm separately, corresponding to the DLS results. The results of particle size increment with encapsulation of DTX, adsorption of siRNA and modification with HA were obtained ($S_{Tab.1}$). Since the anion polymer HA can intensely influence the surface charge of nanoparticles, and the particle size and the excessive positive charge of NPs is an important factor influencing cellular uptake as reported, the particle size and zeta potential changes were measured and recorded by DLS. As shown in Fig. 4, the decreasing zeta potential was observed with the increment of HA component, indicating that the particles were covered with excess negative-charged HA chains. By adding HA to PP and RPSP`NPs, HA was assembled outside and formed the negative shell. Increasing the

dosage of HA, the zeta-potential of PP and RPSP`NPs were decreased. Particle sizes were also determined by DLS (Fig. 4). PP and RPSP`NPs were about 120 nm. With the addition of HA, the size of NPs was enlarged. HPP and HRPSP (N:P:COOH=40:1:16) NPs reached nearly 250 nm. Further increasing the HA dosage, the particle size was decreased. The proper reason was that the zeta potential of HPP and HRPSP NPs were near neutrality due to the electrostatic neutralization between HA and PEI chain. The incompact structure lead to the enlargement of particle sizes. With further increment of HA dosage, the size of HPP and HRPSP`NPs were reduced.

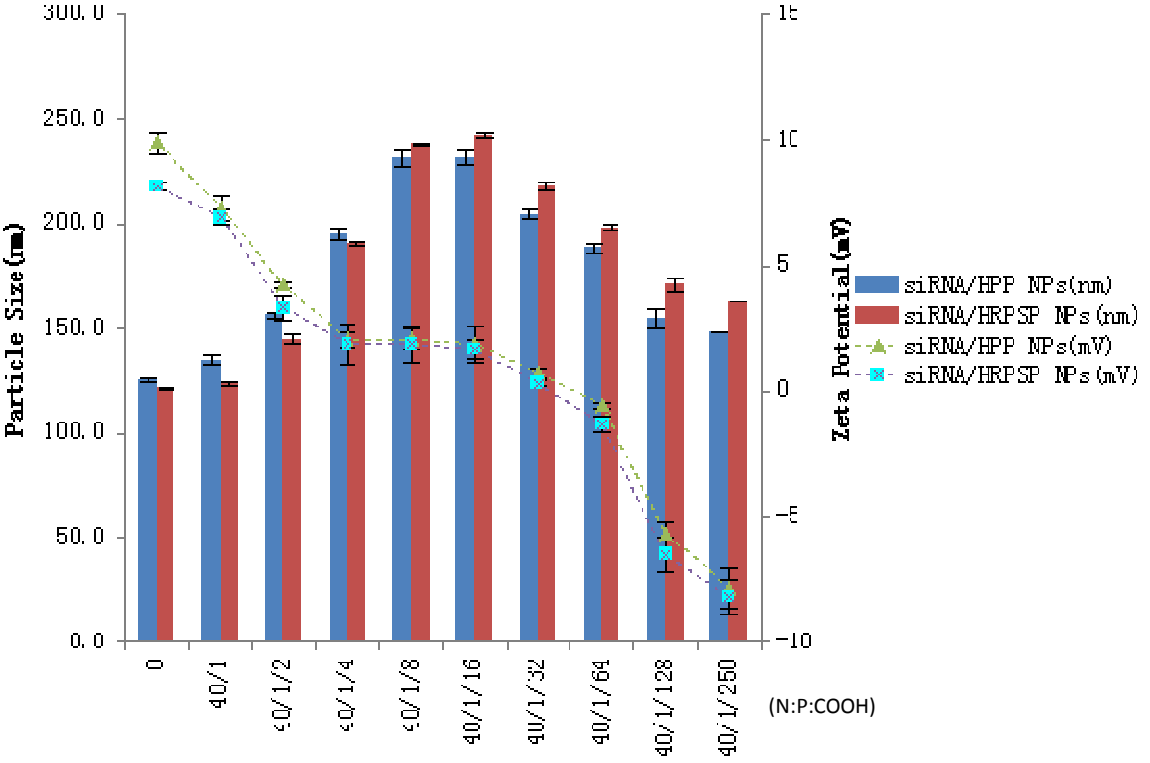

Fig.4. Particle size and zeta potential changes of NPs (N:P:COOH= 40:1:X) with increasing HA dosage.

In vitro cytotoxicity studies

The cytotoxicity effects of free PEI (~1.8kDa,~25kDa), PP NPs, HPP NPs and RPSP NPs, HRPSP NPs as carriers were separately investigated in two cell lines, SGC 7901 and normal cell lines, HMC using MTT assays. Theoretically, the materials used for assembly vectors require low toxicity and much less damage to normal cells. SGC-7901 cell lines which positively express CD_{44} receptors, and normal cell lines, HMC cell lines were both chosen as two experimental objectives. As shown in Fig.5A and Fig.5B, in both cell lines the carrier showed remarkably significant differences in cytotoxicity. PEI with different molecular weight separately possessed the lowest cytotoxicity (Mw 1.8kDa) and the highest cytotoxicity (Mw 25kDa) (Fig.5A). This might be caused by a distinction between their surface charge densities[27]. However, when branched PEI (~25kDa) was prepared into nanoparticles, the cytotoxicity was extremely decreased in contrast to free PEI (~25kDa). Moreover, the cytotoxicity of the nanoparticles based on PLGA and synthesized PEI cross-linked by disulfide bond (RPS) was significantly lower than commercially low molecular weight PEI (~ 25kDa) due to good biocompatibility of RPS as expected. On the other hand, HA modified nanoparticles showed less or similar cytotoxicity compared to the nanoparticles without modification, as a result of

reduced positive charge density. Table 4 summarized the IC_{50} values of PP, HPP, RPSP, and HPRPSP NPs in different cell lines after 24 h incubation. Significantly higher IC_{50} values compared to that of RPSP NPs was observed for HRPSP NPs in different cell lines（$P<0.01$). Interestingly, HPP NPs incubated with both of the subjected cell lines produced a lower IC_{50} value than PP NPs（$P<0.01$）, which indicates that the positive charge decrease might not be the only factor to affect the cytotoxicity. Referring to previous studies [28], the biocompatibility of PEI with cells was thought to be influenced by not only molecular weight, charge density and type of the cationic functionalities, but also by the structure and conformational flexibility. Consequently, in HMC cell lines, it also produces consistent results(Fig.5B). These results suggested that HPRPSP NPs had little cytotoxicity against SGC7901 and HMC cells and were fairly safe to be used as pharmaceutical vehicles.

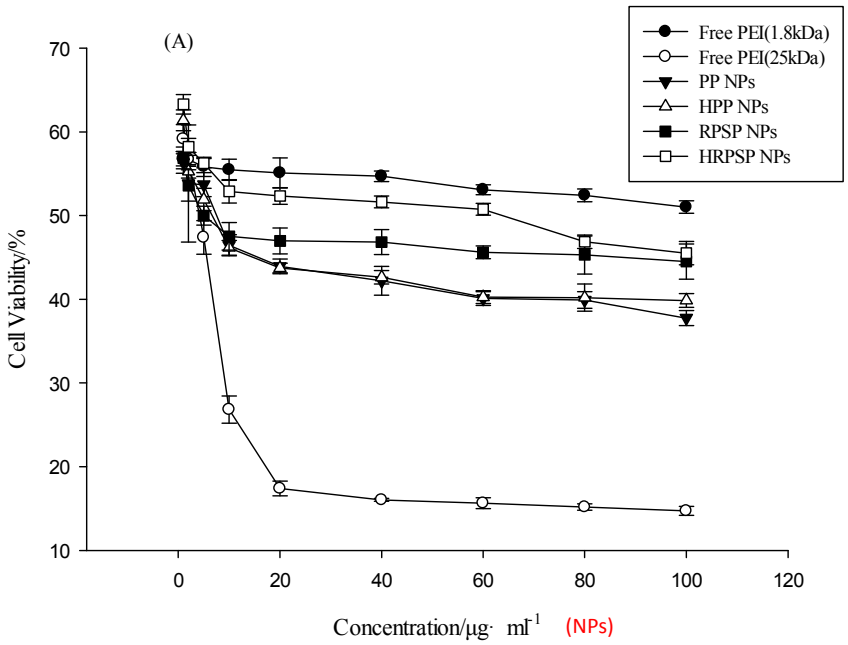

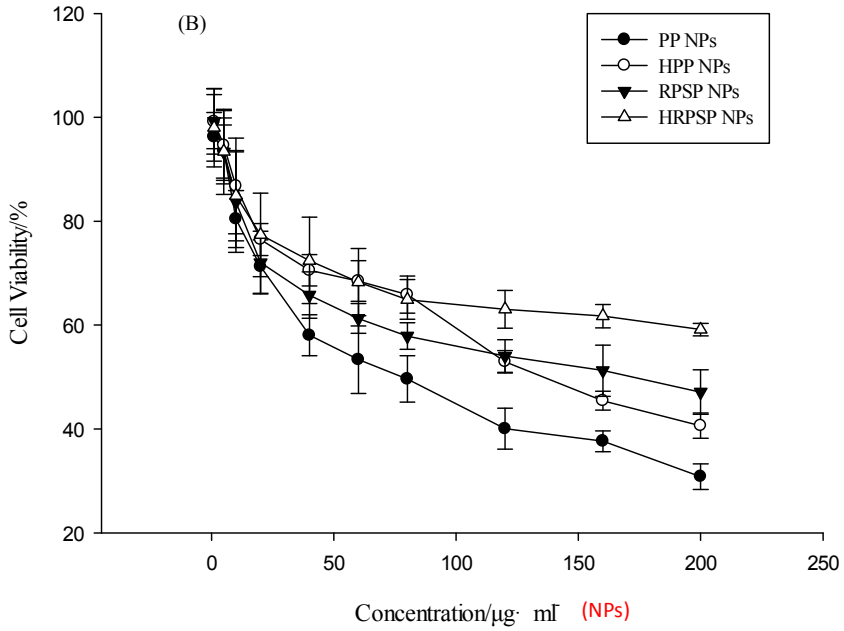

Fig.5 Inhibition rate of carriers to SGC-7901（Fig.5A）, and HMC cell lines (Fig.5B) after incubation for 24h.

Tab.4 IC_{50} value of carriers to SGC-7901 cell lines and HMC cell lines (n=5).

IC_{50} ($\mu g \cdot ml^{-1}$)	PEI (~1.8kDa)	PEI (~25kDa)	PP NPs	HPP NPs	RPSP NPs	HRPSP NPs
SGC-7901	--	14.02±2.63	44.33±5.02	23.18±1.46**	48.56±14.86	71.22±11.88$^{\#}$
HMC	--	--	154.02±25.54	96.25±14.52**	227.90±70.07	446.14±110.83$^{\#\#}$

$^{*}p < 0.05$ and $^{**}p < 0.01$ vs. PP NPs; $^{\#}p < 0.05$ and $^{\#\#}p < 0.01$ vs. RPSP NPs

Results were expressed as the mean±S.D. from five independent experiments.

Formation and stability of PP, HPP, RPSP, and HPRPSP NPs

siRNA condensation is one of the prerequisites for gene transfection. Examined by agarose gel electrophoresis, the migrations of siRNA in agarose gel were completely retarded when the N/P ratio was higher than 10:1 and N/P/COOH was between 10/1/2 and 10/1/24, indicating that all nanoparticles could electrostatically neutralize the siRNA and deter electrophoretic mobility, as shown in Fig.6A, although siRNA could be absorbed on the nanoparticles by electrostatic interaction, the anions existing in the blood could affect the stability through competitive replacement. Heparin was used as an anionic representative to test if the binding ability between them were strong enough. Fig.6B-1 showed that the ratios allowing the dissociation of siRNA in siRNA /PP NPs and siRNA/ RPSP NPs were over 0.15 and 0.25, respectively, illustrating that RPSP NPs could be more protective from heparin than PP NPs. As to siRNA/HPP NPs and siRNA/HRPSP NPs, the similar results were obtained when the corresponding ratios were 0.2 and 0.5, separately. Fig.6B-2 also showed the comparative stability differences between the four NPs groups. Another important factor influencing the stability of siRNA is enzyme degradation. We incubated the complexes with RNase at 37°C for various time periods to observe the degradation of siRNA. In Fig.6C-1, the upper images of every single

figure (1, 2, 3, 4) represent naked siRNA incubated with RNase as the control group, and the images at the bottom are siRNA/NPs. The integration curve (Fig.6C-2) makes it clear that 30% and 15% of siRNA in siRNA/PP NPs and siRNA/ RPSP NPs was degraded during 60 min; inversely more than 90% of naked siRNA was destroyed at the same time. Furthermore, HA contributes to the degradation of almost the entire siRNA in siRNA/HPP NPs and siRNA/HRPSP NPs during 4h. Attributed to the disulfide bonds, siRNA releases more readily from siRNA/RPSP NPs, which was verified by agarose gel retardation (Fig.6D). In comparison to siRNA/PP NPs and siRNA/HPP NPs, siRNA/RPSP NPs and siRNA/HRPSP NPs release the siRNA in advance at heparin/siRNA weight ratios of 0.2 and 0.1. This indicated that disulfide bonds were advantageous to siRNA release.

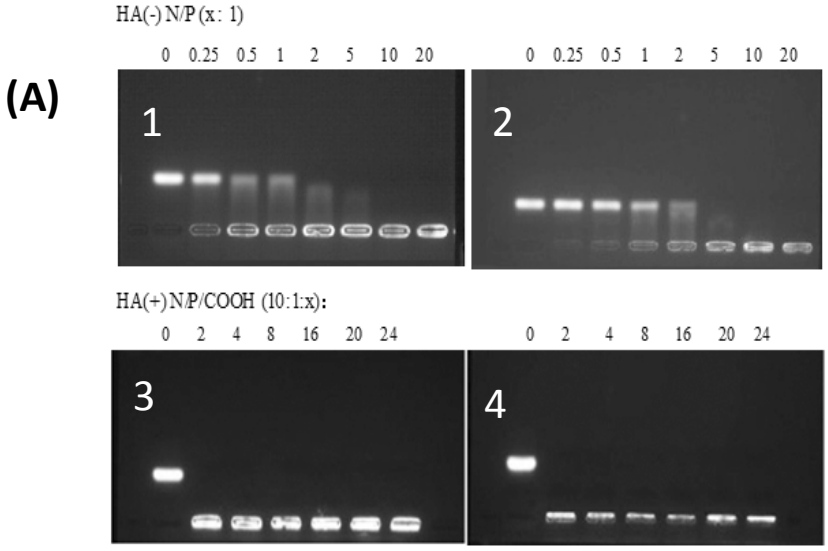

Fig.6A Electrophoretic retardation analysis of siRNA binding by different NPs. The gel results for the individual NPs are shown from (1) to (4): (1) siRNA/PP NPs, (2) siRNA/RPSP NPs, (3) siRNA/HPP NPs, (4) siRNA/HRPSP NPs; Lane numbers were corresponded to different N:P molar ratios from 0 to 20:1. In case of (3) and (4), the lane numbers correspond to different N:P : COOH molar ratios from : 10:1:X(X=0～24)

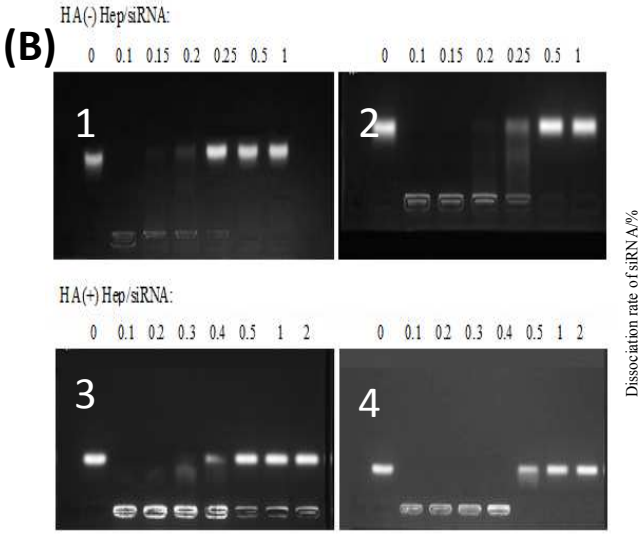

Fig.6B-1

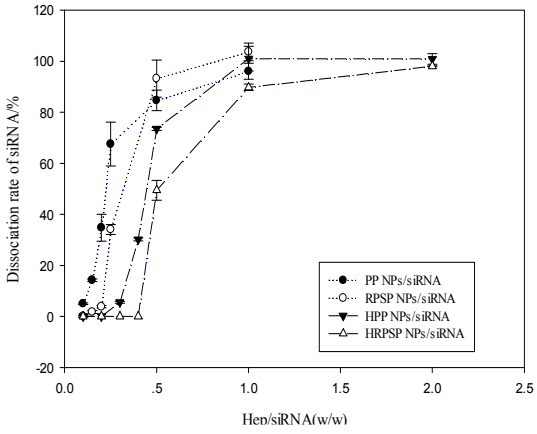

Fig.6B-2

Fig.6B-1 Gel retardation assay of siRNA/NPs or anti-anion replacement capability: (1) siRNA/PP NPs(N:P=10:1), (2) siRNA/RPSP NPs(N:P=10:1), (3) siRNA/HPP NPs(N:P:COOH=10:1:24), (4) siRNA/HRPSP NPs (N:P:COOH=10:1:24); In case of (1) and (2), lane numbers were corresponded to different weight ratio of heparin（hep） to siRNA (w/w) from 0～1 and in case of (3) and (4), lane numbers were corresponded to different weight ratio of heparin（hep）to siRNA (w/w) from 0～2. Fig.6B-2. siRNA dissociation from NPs by heparin competition. The dissociation was determined by assessing free siRNA by agarose gel electrophoresis. The data are represented as mean ± standard error for n = 3.

(C)

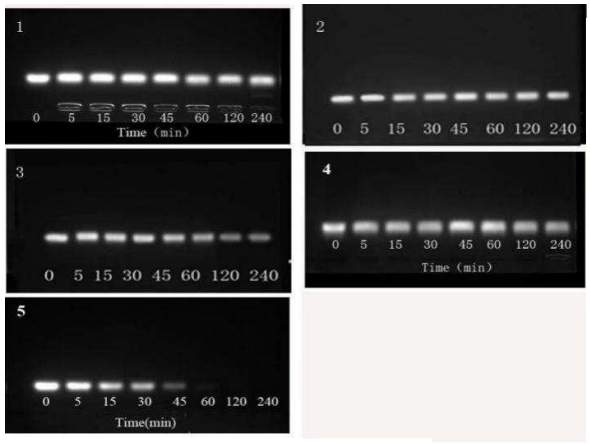

Fig.6C-1

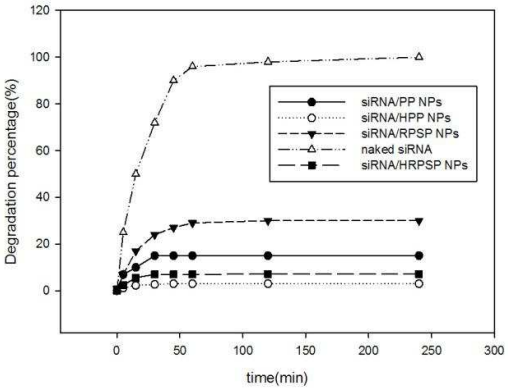

Fig.6C-12

Fig6C-1 Gel degradation assay of siRNA after incubation of siRNA/NPs with RNase for various time periods of 0,5, 15, 30, 45, 60, 120, 240 min. (1) siRNA/PP NPs (N:P=10:1), (2) siRNA/HPP NPs (N:P:COOH=10:1:24), (3) siRNA/RPSP NPs (N:P=10:1)(4) siRNA/HRPSP NPs (N:P:COOH=10:1:24), (5) Naked siRNA. Fig.6C-2 The degradation profile of intact siRNA from NPs compared to naked siRNA in RNase. The data shows the degradation percentage of intact siRNA from carriers.

(D)

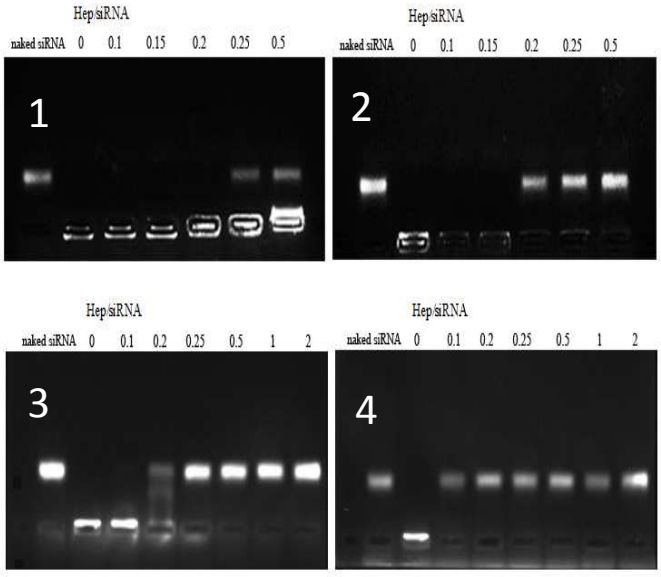

Fig6D siRNA reductable releasing images of (1) siRNA/PP NPs (N:P=10:1), (2) siRNA/RPSP NPs (N:P=10:1), (3) siRNA/HPP NPs (N:P:COOH=10:1:24) and (4) siRNA/HRPSP NPs (N:P:COOH=10:1:24) after being incubated with GSH (0.2mol/L) at 37°C for 24h. In case of (1) and (2), the lane numbers were corresponded to different weight ratio of heparin（hep） to siRNA (w/w) from 0～0.5; In case of (3) and (4), the lane numbers were corresponded to different weight ratio of heparin（hep） to siRNA (w/w) from 0～2.

Intracellular uptake of siRNA/HRPSP NPs

It is well known that the receptor expression levels are critical for cellular entry for systems that are internalized based on receptor recognition . Thus prior to testing the siRNA encapsulated nanosystems in cells for gene silencing activity, the relative amounts of CD44 receptor levels on the surface of SGC-7901 and HMC cells were treated with monoclonal antibody against CD44 receptors to determine the receptor levels on the surface of the cells by flow cytometry.The corresponding cell uptake SGC-7901 and HMC cells were(80.2±3.5)% and (5.8±1.3)% respectively[29].

The siRNA/HRPSP NPs were optimized for in vivo applications in terms of transfection efficiency by adding various proportions of HA (Fig.7). Firstly , the transfection efficiency of siRNA/RPSP NPs in SGC-7901increased gradually within incremental weight ratios of HA and then decreased after the molar ratio of N:P:COOH reached to above 40:1:8. This is may be owing to the reduced positive charge on the complexes which turned into the main factor to enter cells with HA increment. The similar tendency was obtained in siRNA/PP NPs. Because of the most remarkable transfection efficiency, siRNA /HRPSP NPs (N:P:COOH=40:1:2) was exploited for further studies. The uptake of these complexes might be ascribed to the receptor mediated endocytosis of to SGC 7901 cells with HA receptors. The figure shows fluorescence microscopic images reflecting the cellular uptake differences between the CY3-siRNA/HRPSP NPs and CY3-siRNA/RPSP NPs in SGC-7901 cells which corresponband with the above results(S2) . CY3-siRNA/HRPSP NPs was up-taken into SGC-7901 cells more efficiently than CY3-siRNA/RPSP NPs . In addition to that , the histogram shows the RPSP NPs or HRPSP NPs shows slight increasement but no significant differences compared with PP NPs or HPP NPs The possible reason for that may be that disulfide bond can dramatically alter steric hindrance and increase the flexibility of PEIss to contact with the cell membrane for endocytosis and the local electrostatic micro-environment of the disulfide bond can achieve the responsiveness of the disulfide bond to biological stimuli . This deduction need further studies. These results suggest that HRPSP NPs was more easily internalized by the SGC 7901 cells. This could be due to presence of CD44 receptors in these cells [30].

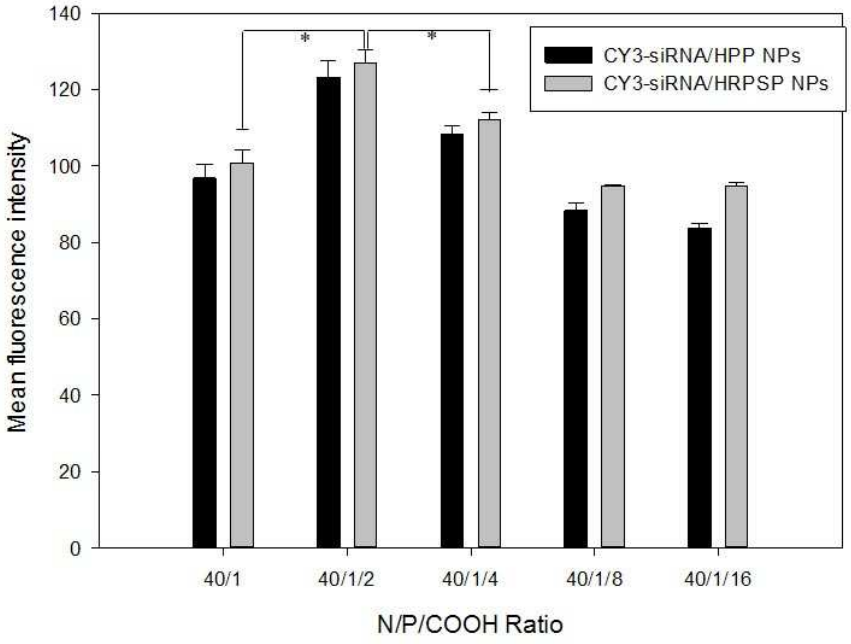

Fig.7 Comparative mean fluorescence intensity of nanocomplexes with increasing HA by FACS.

To confirm the HA receptor mediated endocytosis, the competitive binding assays were carried out. The uptake effect of CY3-siRNA was quantitatively determined using flow cytometric analysis after adding 10mg/ml of free low molecular weight soluble HA (11kDa) in the transfection medium. Cells without any treatment were used as a negative control and that were transfected by siRNA/Lipofectamine® complex as a comparison. As shown in Fig.8, the mean fluorescence intensity of Cy3 from the cells decreased drastically in case of the medium containing free HA ($p \leq 0.01$), while for siRNA/ Lipofectamine® complex there was no significance between the cells with and without saturation with free HA.. It might be explained by the fact that high concentration of free HA molecules pre-dominated the HA receptors like CD_{44} on the SGC 7901 cell surface and reduced the receptor mediated endocytosis of Cy3-siRNA/HPP and Cy3-siRNA/HRPSP NPs. Considering all these results, HA in the outer surface of Cy3-siRNA/HPP and Cy3-siRNA/HRPSP NPs was thought to significantly contribute to the improved cellular uptake by HA receptor mediated endocytosis, making target specific delivery to the tissues possible with HA receptors.

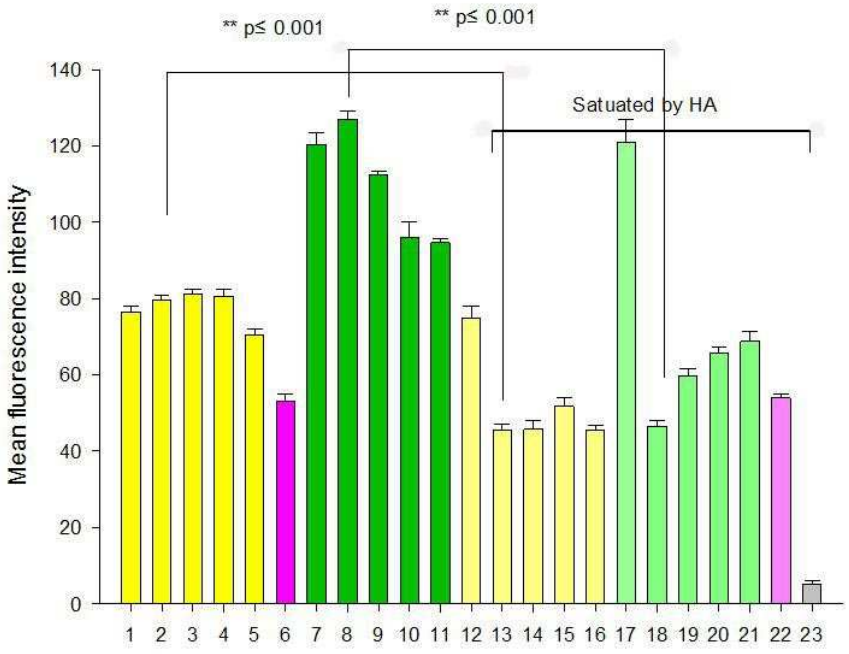

Fig.8 Measured mean fluorescence intensity in SGC-7901 cells after 24h of administration., (1) CY3 siRNA/PP NPs, N/P=40/1; (2~5) CY3 siRNA/HPP NPs, N/P/COOH =40/1/2,40/1/4,40/1/8,40/1/16; (6) Lipofectamine®. (7) CY3 siRNA/ RPSP NPs, N/P=40/1; (8~11) CY3 siRNA/HRPSP NPs, N/P/COOH =40/1/2, 40/1/4, 40/1/8, 40/1/16. Pre-treatment of free HA : (12) CY3 siRNA/PP NPs , N/P=40/1; (13~16) CY3 siRNA/HPP NPs, N/P/COOH= 40/1/2, 40/1/4, 40/1/8, 40/1/16; (17) CY3 siRNA/RPSP NPs, N/P=40/1; (18~21) CY3 siRNA/HRPSP NPs, N/P/COOH=40/1/2, 40/1/4, 40/1/8, 40/1/ 16.(22)Lipofectamine (23)negative control

Mechanism of cellular uptake

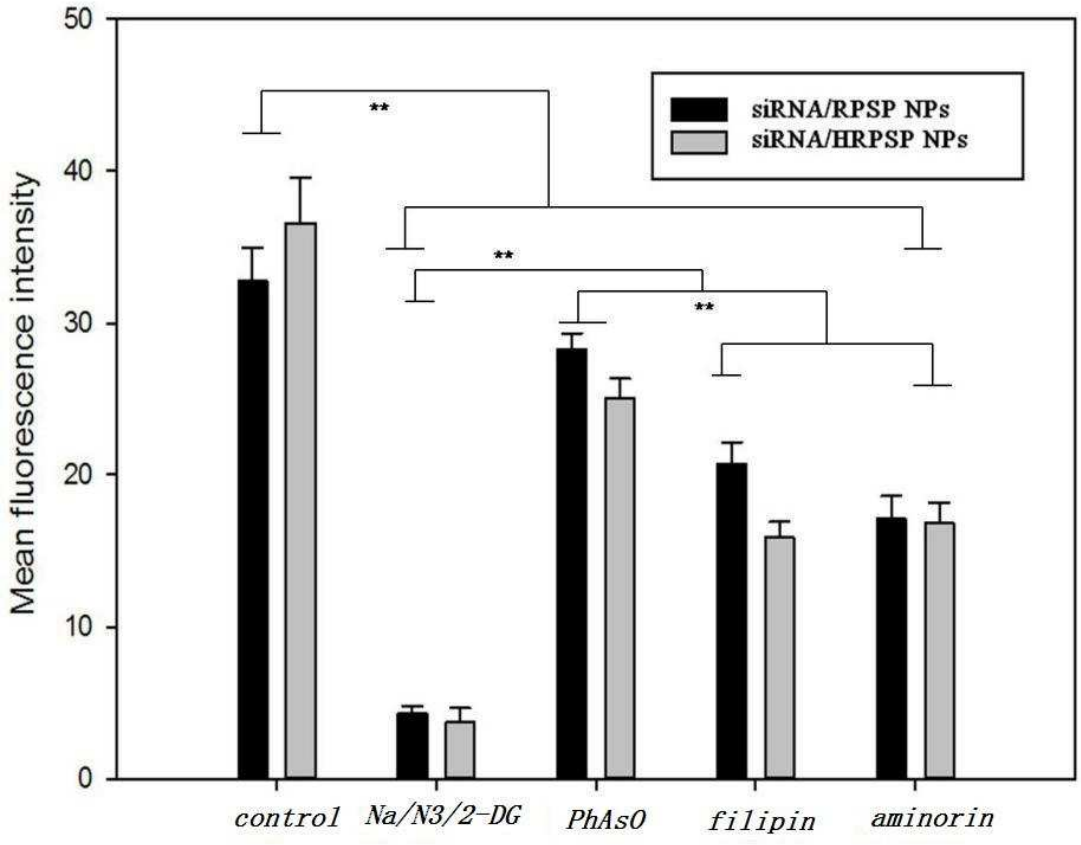

Fig.9 Cellular uptake of siRNA/RPSP and siRNA/HRPSP NPs represented by mean fluorescence intensity (MFI) of FAM-siRNA in the presence of uptake inhibitors. Values are presented as mean ± sd, n=4.

A high cellular uptake and entrapment inside the cells has been clearly demonstrated for the siRNA/HRPSP NPs formulation. The next question to be answered was which kind of mechanism these results can be attributed to. To confirm the routes of particle internalization of the NPs uptake into SGC-7901cells, the cellular uptake was pretreated with different uptake inhibitors. Cellular uptake mechanism is essential to be demonstrated clearly in that whether it is independent from endosomes, and that determines the efficiency of siRNA delivery into the cytosol and subsequently have the gene silencing effect[31]. As reported, chlorpromazine hydrochloride promotes clathrin agglutination in late endosomes which inhibit the formation of endocytosis sag coated with clathrin[32].Filipin is known to interact with cholesterol and has an influence on caveolae-mediated uptake[33]. Nocodazole depolymerizes microtubules which prevents the transport vesicle from fusing with the pre-lysosomal compartments (late endosomes) and protects the contents of the transport vesicles from lysosomal degradation[34]. Aminorin inhibits macropinocytosis by inhibiting the Na+/H+ exchange required for macropinocytosis[35]. For poly(ethylene imine) as a standard transfection agent, two different uptake routes, a clathrin- and a caveolae-dependent one, are known[36].

The cellular uptake of nanoparticles is an active and energy-intensive process, and the required energy can be produced by aerobic oxidation of mitochondria and glycolysis in the cytoplasm. The former process is the primary source of energy. Sodium azide (NaN3) can inhibit the production of energy by blocking the respiratory chain of mitochondria. Therefore, it is widely used to research the energy dependence of cells.The influence of energy on cellular uptake is shown in Fig.9. A decreasing MFI was observed in SGC7901 cells incubated with

NaN3/2-DG (P<0.01), which suggests that energy generated by aerobic breathing could more effectively influence uptake of HRPSP/siRNA and RPSP/siRNA NPs in SGC 7901 cells.Cell-associated fluorescence was significantly decreased after incubation in the presence of filipin, chlorpromazine and aminorin, demonstrating an inhibition of particle uptake (Fig.8, t-test, p<0.001). These data indicate that the cellular uptake of HRPSP/siRNA and RPSP/siRNA NPs was relevant with caveolae, clathrin and macropinocytosis pathways. In case of HRPSP/siRNA NPs, phAsO, filipin and aminorin inhibited internalization by 20% (P < 0.01), 60% (P < 0.01) and 50% (P<0.01), respectively. Therefore, we can conclude according to the above experimental results that for HRPSP/siRNA and RPSP/siRNA NPs, clathrin-mediated uptakepathway is not the primary uptake pathway in SGC-7901 cells.

Taken together, the result of the cellular uptake mechanism studies suggest that the caveolae-mediated endocytosis and endocytosis are the major cellular uptake pathways for HRPSP/siRNA and RPSP/siRNA NPs; whereas, clathrin-mediated endocytosis is the following routes of HRPSP/siRNA and RPSP/siRNA NPs internalization. Caveolae-mediated endocytosis is not associated with a pH decrease, and is known to be a non-digestive route of external substances into the cellular compartment[37,38]. Thus, HRPSP/siRNA and RPSP/siRNA NPs internalized by caveolae- mediated endocytosis may be able to avoid siRNA degradation in acidic organelles, leading to higher transfection and gene silencing efficiency.

The inhibitory effect on COX-2 expression

As shown in Fig. 10 (A), in vitro gene silencing of siCOX-2 was assessed in SGC-7901 cells. After treatment with NPs/siCOX-2 complex, COX-2 mRNA expression was reduced to a statistically significant level, whereas no significantgene silencing was observed with scrambled HRPSP/siRNA complex control and negative control, suggesting that the gene knockdown was only induced by COX-2 siRNA alone. siCOX-2/HPRSP NPs resulted in statistically more significant decrease of COX-2 mRNA expression level than siCOX-2/PP and siCOX-2/RPSP complexes. Approximately 2-fold reduction of COX-2 mRNA level was observed after treatment with siCOX-2/HPRSP NPs compared with siCOX-2/HPP NPs (P<0.01), and 3-fold reduction compared with siCOX-2/Lipofectamine NPs(P<0.01). As shown in Fig.10B, all these siRNA complexes down-regulated COX-2 gene expression. DTX/siCOX-2/HRPSP NPs had comparable efficiency to lipofactamine and showed the best silencing efficiency that is 77% at the protein (P<0.01 compared with negative control and other complexes), indicating that DTX/siCOX-2/HRPSP NPs could enhance down-regulating the expression of COX-2 protein. These results suggest that efficient down-regulation of COX-2 protein is likely due to the efficient cell uptake, intracellular release of siRNA. Besides, Mariana Lemos Duarte et al[39] proved that COX-2 mRNA in A549 cells and H460 cells treated by paclitaxel for 48h up regulated significantly 7~30 times, and less 7 times for 24h, which indicated the upregulation degree was relevant with incubation time length. Taken this together，it is rational to presume the synergy effects of COX-2 siRNA and DTX will be much more significant with time extension. Certainly, in our study, the mechanical insights on synergistic effects between DTX and siCOX-2 needs further research to be confirmed.

(A)

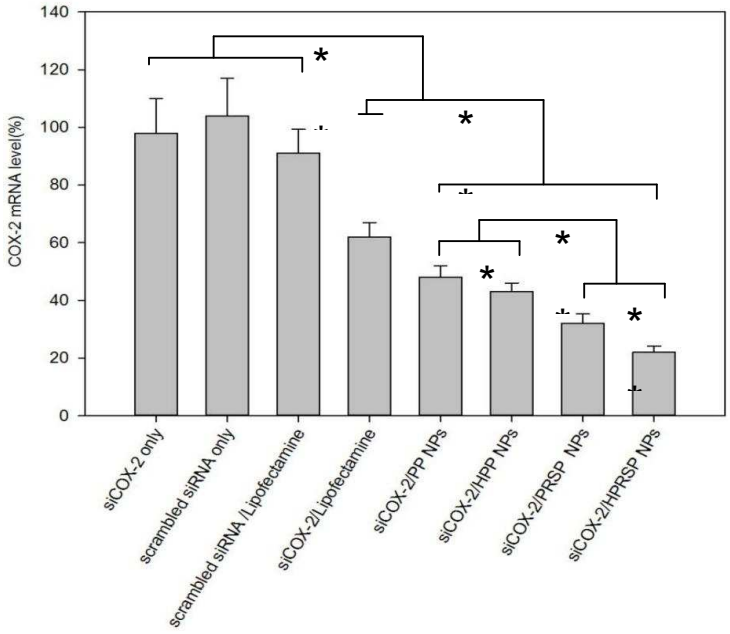

(B)

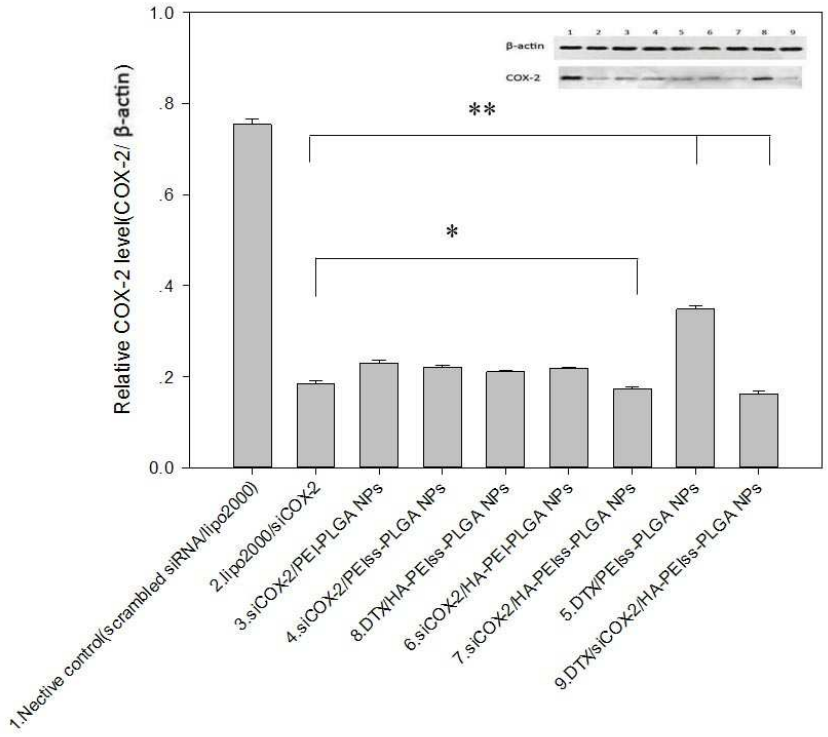

Fig.10(A) Expression of COX-2 mRNA determined by RT-PCR. (B) Densitometry analysis of Western blots following COX-2 knockdown.

The upper right corner showed the analysis of light intensities of COX-2 protein expression from Western blot results; lane 1: Negative Control NPs (NC-NPs); lane2: siRNA/Lipo®2000; lane3: siRNA/PP NPs; lane 4: siRNA/RPSP NPs; lane 5: DTX/RPSP NPs; lane 6: siRNA/HPP NPs; lane 7: siRNA/HPRPSP NPs; lane 8: DTX/HPRPSP NPs; lane 9:siRNA/DTX/HPRPSP NPs;. SGC-7901 cells were transfected with siRNA/NPs at N/P of 40:1 and N/P/COOH of 40:1:2. The concentrations of siRNA-COX-2 with Lipofectamine 2000® (siRNA/ Lipo2000®) and NC were 100nM. Transfection experiments were performed independently three times. *$p<0.05$, **$p<0.001$ as compared with controls (n=3).

In vivo imaging analysis

To evaluate the biodistribution of siRNA/PP NPs, siRNA/HPP NPs, siRNA/RPSP NPs, siRNA/HRPSP NPs,, the DiI -labeled complexes were i.v. injected into tumor-bearing mice. Fig.11 A shows the real-time images of the four types of NPs in the tumor-bearing mice, in which the whole bodies of live mice were monitored at 2 h, 4h and 8 h after administration by a non-invasive near infrared optical imaging technique, respectively. A stronger fluorescent signal detected in the tumor region in mice treated with the complex was due to an enhanced permeability and retention (EPR) effect[40]. The complex modified by HA enhanced higher tumor targeting efficiency by the targeted CD44 receptor-mediated uptake of NPs. Then gained the tumor and organs after 8h in Fig11B. Fig. 11C shows the values of the fluorescence intensity. In the quantitative analysis (Fig. 11C), HPRSP NPs exhibited more than 1.5-fold higher intensity at the tumor tissue compared to siRNA/HPP NPs, 2-fold higher intensity compared to siRNA/RPSP NPs and 3-fold higher intensity compared to siRNA/PP NPs, owing to the reduction that trigered intracellular release of NPs, which could reduce the elimination of complex and exhibited a prolonged circulatory and hence prolonged the retention of Dir in tumor site. However, the intensity in liver and kidney significantly increased with HPRSP NPs compared to siRNA/RPSP NPs because of the homeostasis of HA in the body known to bemaintained by the receptor mediated HA degradation inthe liver and kidney. The tumor-to-normal tissue (T/N) distribution ratios of DTX are summarized in S_{Tab2}. The tumor-to-normal tissue (T/N) distribution ratios show that the accumulation in tumor with siRNA/HRPSP-Dir NPs is 6.22 folds higher than brain, versus 5.51 with siRNA/RPSP-Dir NPs and 2.23 with siRNA/PP-Dir NPs, indicating the enhanced targeting to tumor. The distribution pattern observed was consistent with the other organs (heart, liver, spleen, lung and kidney). Overall, in vivo biodistribution studies indicate that HRPSP NPs can be expected to be highly efficient drug delivery vehicles to achieve targeted co-delivery of gene and small anti-cancer drugs.

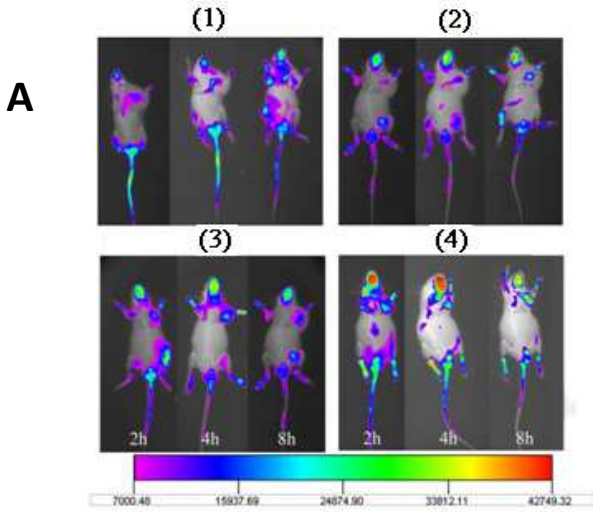

C

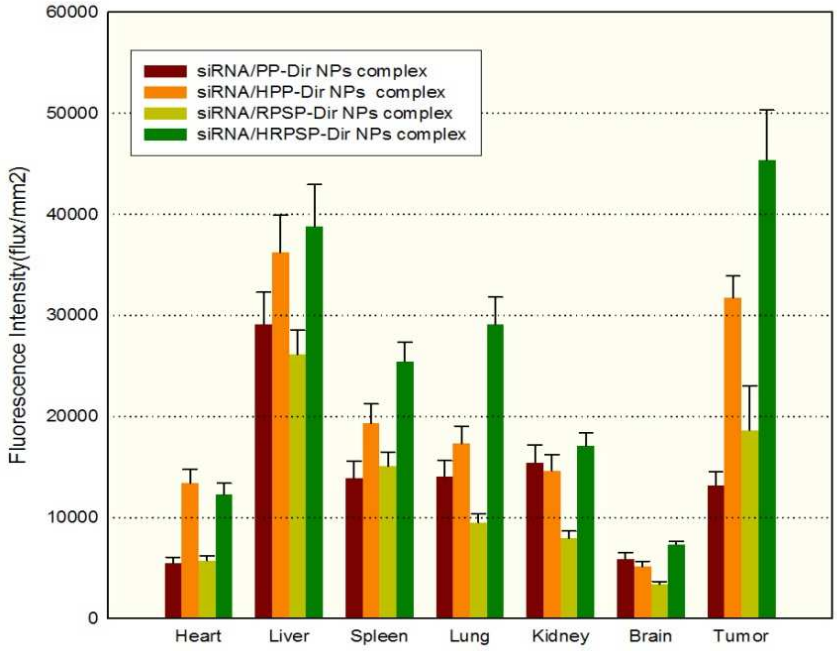

Fig.11(A) In vivo imaging of tumor-bearing mice after administration of Dir and siRNA loaded co-delivery NPs at 2h, 4 h, 8 h from left to right; 1:PP, 2: HPP;3: RPSP; 4: HPRPSP. (B) Ex vivo fluorescence images of tissues including heart, liver, spleen, lung, kidney and tumor collected at 8 h post-injection of Dir and siRNA loaded co-delivery nanoparticles. 1. Dir/PP NPs/siRNA; 2. Dir/siRNA HPP NPs; 3. Dir/RPSP siRNA NPs; 4. Dir/siRNA/HRPSP NPs. (C) Quantification of the ex vivo tissue uptake characteristics of NPs in tumor-bearing mice after 8h post-injection. Uptake expressed as photoflux per mm2 of tumor.

In vivo Biodistribution study

The DTX was detected in tumor lysates but at a lower level compared to liver in the four groups after 10min, indicating the period was so short that the drug distribution in tumor tissues has not reached equilibrium yet. Interestingly, DTX amount in tumor revealed that the mice treated with DTX/HPP NPs and DTX/HRPSP NPs presented significantly higher DTX accumulation intumor site at 1.0h(Fig.12B) and 12h(Fig.12C) compared with DTX/PP NPs and DTX/RPSP NPs corresponding with the transfection results . The levels detected in liver with DTX/RPSP NPs and DTX/HRPSP NPs were lower than DTX/PP NPs and DTX/HPP NPs, suggesting the decreased uptake by hepatic cell and the efficient targeting in tumor ($P<0.01$). Moreover, lower DTX levels were observed for DTX/HRPSP NPs in the lung compared to other groups which might be attributed to the shelter of positive charge by HA which reduced the accumulation in lungs ($P<0.01$). Taking the negatively charged surface and nanoscale size of the nanocomplexes, it should prefer to stay in blood with prolonged retention time which leads to the accumulation in tumor by the over-expressed receptor endocytosis. These collected data demonstrated that DTX/HRPSP NPs

could in general reduce DTX uptake by healthy organs tissues, particularly the liver and lung, to limit the side effects while significantly increasing DTX accumulation in tumors.

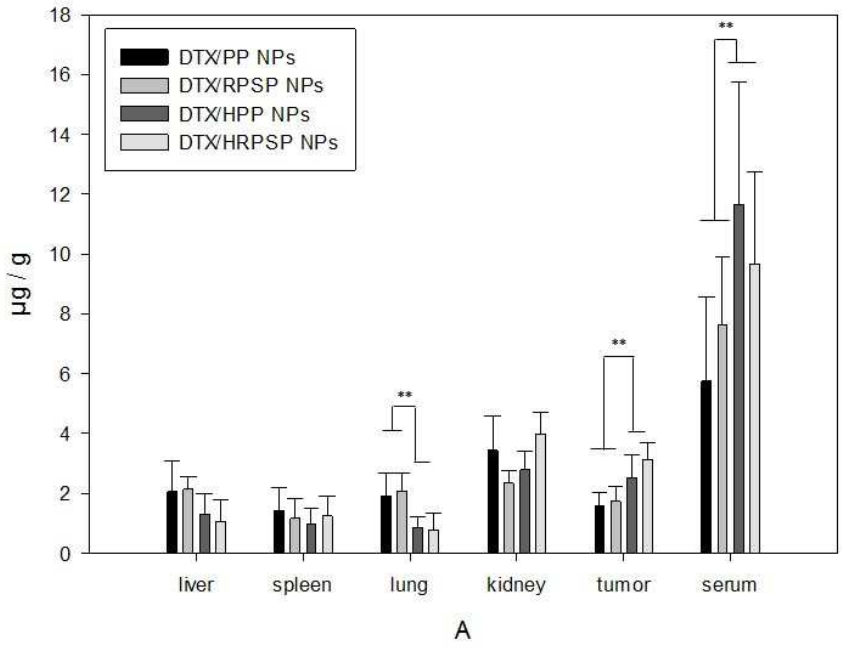

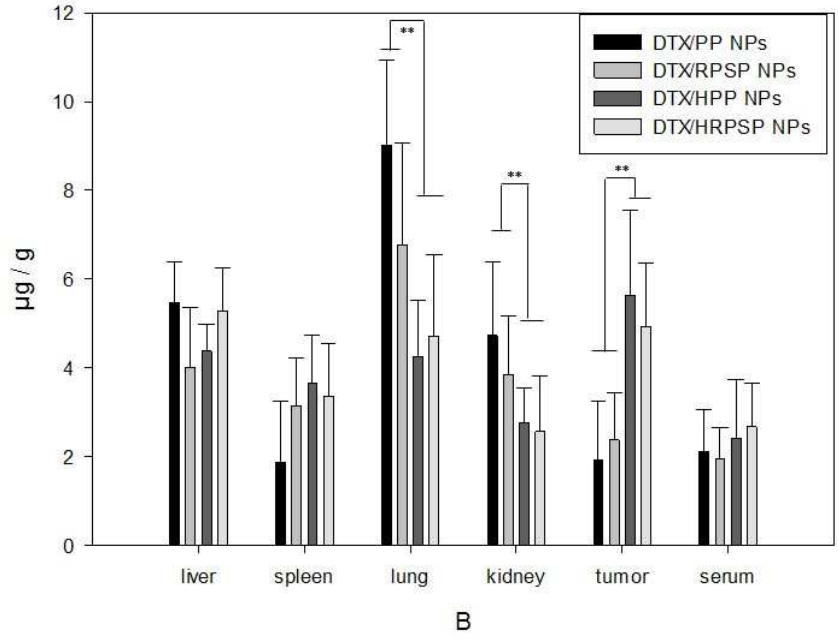

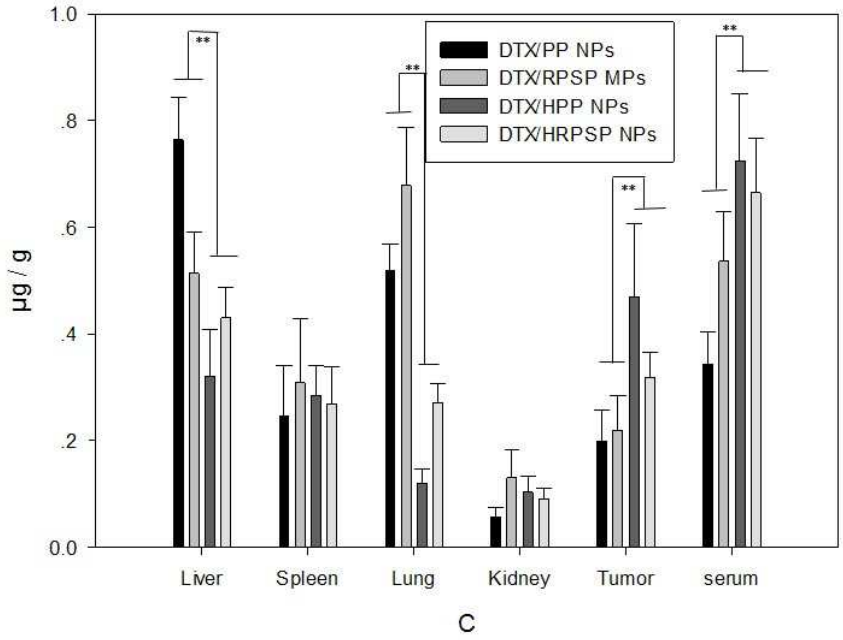

Fig.12 Biodistribution of DTX/PP, DTX/HPP, DTX/RPSP, DTX/HRPSP formulations after tail-vein injections to tumor-bearing nude mice. Afteranatomization in 10min（A）, 1h（B） and 12 h（C）, the amount of DTX in dissected tissues was determined by HPLC and expressed as a percentage to the amount of DTX according to the amount per gram of tissue (μ g/g). Data are represented in Tab.4 as a mean±SD （n = 3）. ** P <0.01 compared to PPNPs and HPP NPs.

Tab.5 The $AUC_{0\text{-}12h}$ and Te of tumor-bearing nude mice tissues in each formulation (n=6).

Tissue	DTX/HPP NPs		DTX/HRPSP NPs	
	AUC（$\overline{X}$ ± SD）（h •μg/g）	T_e（$\overline{X}$ ± SD）	AUC（$\overline{X}$ ± SD）（h •μg/g）	T_e（$\overline{X}$ ± SD）
Liver	28.85±4.37	0.183±0.031	34.519±4.87	0.209±0.028
Spleen	24.00±3.91	0.148±0.025	22.469±3.21	0.127±0.024
Lung	26.61±3.52	0.167**†±0.023	30.041±4.93	0.177**†±0.031
Kidney	19.70±4.02	0.118**†±0.028	19.611±3.86	0.109**†±0.021
Tumor	38.24±5.29	0.259**†±0.037	33.908±5.21	0.204**†±0.018
Serum	30.96±5.31	0.20±0.031	29.951±4.43	0.176±0.020
Tissue	DTX/PP NPs		DTX/RPSP NPs	
	AUC（$\overline{X}$ ± SD）（h •μg/g）	T_e（$\overline{X}$ ± SD）	AUC（$\overline{X}$ ± SD）（h •μg/g）	T_e（$\overline{X}$ ± SD）
Liver	39.14±5.82	0.265±0.031	28.405±4.71	0.215±0.026
Spleen	14.329±3.62	0.083±0.017	21.308±3.21	0.153±0.021
Lung	58.663±8.18	0.458±0.024	45.519±6.38	0.395±0.041
Kidney	33.134±4.27	0.216±0.037	25.781±4.27	0.191±0.031

Tumor	14.599±3.81	0.085±0.013	16.903±3.87	0.118±0.027
Serum	26.771±4.12	0.167±0.021	22.772±3.71	0.165±0.021

*P<0.01 vs DTX/PP NPs; †P<0.01 vs DTX/RPSP NPs

Conclusion

Hyaluronic acid modified disulfide-crosslinked PLGA-PEI nanoparticles (HPRSP NPs) were successfully developed as a target specific and non-toxic co-delivery system of siRNA therapeutics and chemotherapeutics. PEI-SS prepared by the crosslinking of non-toxic low MW PEI (1800Da) with CBA was further coated with HA by electrostatic interaction in the form of HPRSP. The cytotoxicity of HPRSP appeared to be negligible likely due to the degradation of PEI-SS to low MW PEI in the cytosol. The effective cellular uptake of siRNA/HPRSP NPs by HA receptor mediated endocytosis was confirmed by flow cytometric and confocal microscopic analyses. More importantly, the co-delivery system was superior to the siRNA only loaded system and DTX only loaded system, respectively in gene silencing efficiency. Therefore, the co-delivery NPs were found promising in combination therapy of cancer with therapeutic siRNA and chemotherapeutics. There is still further research space (such as pharmacokinetics and pharmacodynamics studies of DTX loaded HRPSP/ siRNA NPs) to make the studies more persuasive and affirm its foundation for further clinical application.

Acknowledgments

This work was supported by the National Natural Science Funds for Young Scholars (81201182), the Doctoral Fund of Youth Scholars of Ministry of Education of China (20130096120003), and the Fundamental Research Funds for the Central Universities for cultivation project （JKPZ2013006）

Notes and references

1 A. Arora, E.M. Scholar ,Role of tyrosine kinase inhibitors in cancer therapy . J. Pharmacol. Exp. Ther., 315 (2005), pp. 971–979

2 R.B. Ewesuedo, M.J. Ratain . Principles of cancer chemotherapy . Oncologic Therapeutics, (2003), pp. 19–66

3 Early Breast Cancer Trialists' Collaborative Group . Polychemotherapy for early breast cancer: an overview of the randomized trials . Lancet, 352 (1998), pp. 930–942

4 Jing Li, Yan Wang, Yu Zhu, David Oupický. Journal of Controlled Release 172 (2013) 589–600.

5 Cuifang Zheng, Mingbin Zheng, Ping Gong, Jizhe Deng, Huqiang Yi,Pengfei Zhang. Biomaterials 34 (2013) 3431-3438.

6 Chunxi Liu, Fengxi Liu, Lixia Feng, Min Li, Jian Zhang, Na Zhang. Biomaterials 34 (2013) 2547-2564.

7 Dai W et al.Pharm Res 2012, 29:2902-2911.

8 Anat Eldar-Boock, Dina Polyak, Anna Scomparin and Ronit Satchi-Fainaro. Current opinion in biotechnology.

9 Wen-Pin Su, Fong-Yu Cheng, Dar-Bin Shieh, Chen-Sheng Yeh, Wu-Chou Su. International Journal of Nanomedicine.

10 Yi Shu,FengmeiPi, Ashwani Sharma,MehdiRajabi,FarzinHaque,DanShu, Markos Leggas,B. Mark Evers, Peixuan Guo. Advanced Drug Delivery Reviews 66 (2014) 74–89.

11 Chan MW, Wong CY, Cheng AS，et al. Targeted inhibition of COX-2 expression by RNA interference suppresses tumor growth and potentiates chemosensitivity to cisplatin in human gastric cancer cells. Oncol Rep. 2007,18(6):1557-6.

12 Foster J,Black J,LeVea Cet al.COX-2 expression in hepatocellular carcinoma is an initiation event;while EGF receptor expression with down-stream pathway activation is a prognostic predictor of survival[J].Ann Surg Oncol,2007; 14(2):752-758.

13 Zamore PD, et al. RNAi: double-stranded RNA directs the ATP-dependent cleavage of mRNA at 21 to 23 nucleotide intervals. Cell, 2000, 101: 25-33.

14 Paddison PJ, et al. Stable suppression of gene expression by RNAi in mammalian cell. PNAS, 2002, 99 (3): 1443-1448.

15 Karagiannis TC, El-Osta A. RNA interference and potential therapeutic applications of short interfering RNAs. Cancer Gen Therapy, 2005,12(10):787-795.

16 Kawakami S, Hashida M. Targeted delivery systems of small interfering RNA by systemic administration. Drug Metab Pharmacokinet. 2007,22(3):142–151.

17 N. Maurer, K.F. Wong, H. Stark, L. Louie, D. McIntosh, T. Wong, P. Scherrer, S.C. Semple, P.R. Cullis. Spontaneous entrapment of polynucleotides upon electrostatic interaction with ethanol-destabilized cationic liposomes . Biophys. J., 80 (2001), pp. 2310–2326

18 .T.M. Allen, C. Hansen, F. Martin, C. Redemann, A. Yau-Young .Liposomes containing synthetic lipid derivatives of poly(ethylene glycol) show prolonged circulation half-lives in vivo . Biochim. Biophys. Acta, 1066 (1991), pp. 29–36

19 S.Y. Jeon, J.S. Park, H.N. Yang, D.G. Woo, K.H. Park . Co-delivery of SOX9 genes and anti-Cbfa-1 siRNA coated onto PLGA nanoparticles for chondrogenesis of human MSCs Biomaterials, 33 (17) (2012), pp. 4413–4423

20 Dawen Dong,Wei Gao, ,Yujie Liu, ,Xian-Rong Qi. Therapeutic potential of targeted multifunctional nanocomplex co-delivery of siRNA and low-dose doxorubicin in breast cancer 。Cancer Letters , 2015, 359（2）：178–186

21 F. Greco, M.J. Vicent . Combination therapy: opportunities and challenges for polymer-drug conjugates as anticancer nanomedicines . Adv. Drug Deliv. Rev, 61 (2009), pp. 1203–1213

22 N. Cao, D. Cheng, S. Zou, H. Ai, J. Gao, X. Shuai . The synergistic effect of hierarchical assemblies of siRNA and chemotherapeutic drugs co-delivered into hepatic cancer cells . Biomaterials, 32 (2011), pp. 2222–2232

23 Hyun-Jong Cho, Hong Yeol Yoon, Heebeom Koo et al . Biomaterials 32 (2011) 7181-7190.

24 Cai S, Xie Y, Bagby TR,et al.J Surg Res, 2008, 147: 247-252.

25 Ji-Zhe Deng, Yun-Xia Sun, Hui-Yuan Wang, Cao Li, Fu-Wei Huang, Si-Xue Cheng, Ren-Xi Zhuo, Xian-Zheng Zhang, Acta Biomaterialia 7 (2011) 2200–2208.

26 Martin Piest, Johan F.J. Engbersen . Journal of Controlled Release 148 (2010) 83–90.

27 Dagmar Fischer, Thorsten Bieber, Youxin Li, Hans-Peter Elsässer, Thomas Kissel.Pharmaceutical Research.16(1999)1273-1279.

28 Jeong-Hun Kang, Yoichi Tachibana,Wakako Kamata et al..Bioorganic & Medicinal Chemistry.18 (2010) :3946–3950.

29 Kim TH, Nah JW, Cho MH, Park TG, Cho CS J Nanosci Nanotechnol 2006;6:2796-803.

30 Y.F. Li, B. Xiao, S.F. Tu, Y.Y. Wang, X.L. Zhang. Braz. J. Med. Biol. Res., 45 (2012), pp. 197–204

31 Mariana Lemos Duartea, Emanuela de Moraes, Elizangela Pontes, et al. Cancer Letters,279 (2009) 57–64.

32 Peifeng Liu, Yanming Sun, Qi Wang, Ying Sun,HeLi, Yourong Duan. Biomaterials, (2013) 1-11.

33 J.E. Schnitzer, P. Oh, E. Pinney, J. Allard, Cell Biol. 127 (1994) 1217–1232.

34 Ulrich S. Huth, Rolf Schubert, Regine Peschka-Süss.Journal of Controlled Release,110 (2006) 490-504.

35 L.J. Hewlett, A.R. Prescott, C. Watts Cell Biol. 124 (1994) 689–703.

36 Markus Benfer, Thomas Kisse.European Journal of Pharmaceutics and Biopharmaceutics.

37 R.G. Parton, K. Simons, The multiple faces of caveolae, Nat. Rev. Mol. Cell Biol. 83(2007) 185–194.[15]

38 P.U. Le, I.R. Nabi, Distinct caveolae-mediated endocytic pathways target the golgi apparatus and the endoplasmic reticulum, J. Cell Sci. 1166 (2003) 1059–1071

39 Mariana Lemos Duartea, Emanuela de Moraes, Elizangela Pontes, et al. Role of p53 in the induction of cyclooxygenase-2 by cisplatin or paclitaxel in non-small cell lung cancer cell lines[J]. Cancer Letters, 279 (2009) 57–64.

40 B.A.Teicher. Drug Resistance Updates,3(2000),pp,67-73